Design of an Actuation Mechanism for Compliant-Body Biomimetic Robots

by

Sean Andrew Mellott

Submitted to the Department of Mechanical Engineering
in partial fulfillment of the requirements for the degree of

Bachelor of Science in Mechanical Engineering

at the

MASSACHUSETTS INSTITUTE OF TECHNOLOGY

June 2009

Author .....
Department of Mechanical Engineering
May 8, 2009

Certified by .....
Kamal Youcef-Toumi
Professor of Mechanical Engineering
Thesis Supervisor

Accepted by .....
J. Lienhard V
Collins Professor of Mechanical Engineering; Chairman,
Undergraduate Thesis Committee

Design of an Actuation Mechanism for Compliant-Body Biomimetic Robots

by

Sean Andrew Mellott

Submitted to the Department of Mechanical Engineering
on May 8, 2009, in partial fulfillment of the
requirements for the degree of
Bachelor of Science in Mechanical Engineering

Abstract

In this thesis, I designed and simulated an actuator mechanism for generating a moment within a compliant (soft) body system. The moment produces vibrational waves throughout a compliant material, and these vibrations are utilized to create biomimetic locomotion. The prototype actuator was developed for use in a fish tail, but it is hope that the actuation system can be applied in other robotic structures. The primary goals of this project included making gains in energy efficiency over previous embodiments, creating a compliant actuator that does not interfere with the natural body vibrations, and creating a system that can easily be modified to be used in a wide variety of soft-bodied systems. The system is also scalable to the size of the structure being actuated.

Thesis Supervisor: Kamal Youcef-Toumi
Title: Professor of Mechanical Engineering

Contents

List of Figures

List of Tables

Chapter 1

Introduction

As society becomes ever more technologically advanced, electromechanical systems are playing an increasingly important role in performing hazardous tasks, tasks that humans otherwise could not perform, and even mundane tasks such as household chores [1]. Not only should robotic systems be able to perform these tasks, but they should be able to do so as reliably and as robustly as possible. One of the primary areas of focus for any robotic system is its means of locomotion. Recent advances in robotics have led to the development of compliant-bodied systems. The advantage of using a compliant body is that the number of actuators needed to create locomotion can be reduced since the compliant material transmits waves and motion through the entire body [2]. This thesis is focussed primarily on the development of an actuator system for a compliant-bodied, robotic fish, although the actuation system can also be applied to other compliant structures with minimal modifications. The compliant fish design was created by Pablo A. Valdivia y Alvarado in his Doctoral Thesis, "Design of Biomimetic Compliant Devices for Locomotion in Liquid Environments [3]." The actuator and associated mechanisms developed within this thesis are designed to be more efficient than designs currently in use, while utilizing small movements to create large, locomotion-inducing vibrations in a synthetic, compliant tail.

1.1 Motivation

The field of robotics is undergoing rapid change as technology continues to allow the development of ever more complex systems. One of the fastest growing areas of development is biomimetics, in which robots are designed with the intention of mimicking nature. However, mimicking natural systems presents an enormous challenge to any designer as nature has had millions of years to develop the complex mechanisms present in the bodies of animals. Take for example, the human arm. From the shoulder to the wrist, it has 7 degrees of freedom. To mimic such motion, traditional modern design would require a skeletal system of complex linkages, joints, hinges, cables, pulleys and up to 7 different actuators. Even slightly more advanced designs, which may utilize improvements such as under-actuated systems and the latest developments in actuation, would still require multiple parts and would require a high degree of mechanical complexity.

In a similar sense, previous embodiments of biomimetic fish motion have involved using forces to push or pull a series of rigid mechanical joints inside of a protective, flexible housing. Examples include both robotuna I and II, which use a system of articulated linkages (composing a spine) and a system of flexible ribs [4]. Each link or joint must be pulled or pushed in order to generate motion. While this system does generate locomotion, it is not the most efficient transfer of power since there are inherent losses from friction and other forces at points where different mechanical parts interface including belts and pulleys, gears, linkages, and other systems. In addition, many of the motors are oscillating, rather than turning in a single direction. Their start and stop motion further reduces their efficiency.

Often the best solution to the problem of developing a robust system is simply to reduce the number of moving mechanical parts. Fewer parts means that fewer failure modes can exist. Biomimetic robotics has developed many novel ways to reduce complexity including using compliant-bodied robots. A compliant-bodied system replaces joints, linkages, cables, pulleys, and actuators with silicone and rubber based composite materials. Because these materials readily distribute energy throughout

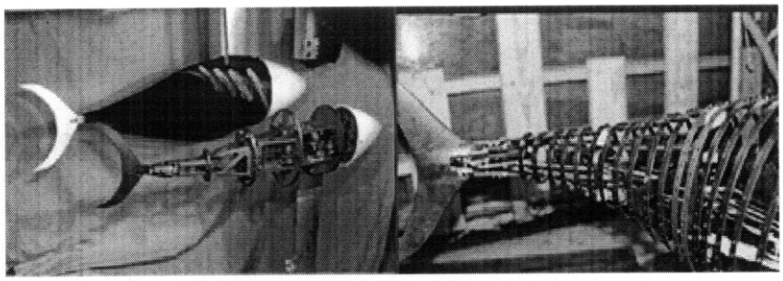

Figure 1-1: Interior view of robotuna I (right) and robotuna II (left) Both systems use a series of actuated linkages to propel themselves forward [5].

their structures, a force or moment generated in one area can create larger effects elsewhere in the structure because the energy travels through the material in waves. Complex motions can be reduced to simple forces and moments perpetuated through a body by vibrations and waves.

1.1.1 Compliant actuation

From looking at the reduction in complexity and in the number of required parts, it is obvious that compliant bodies have certain advantages over more traditional robotic designs. Because the body of the fish will be compliant, it only makes sense that an actuation method should also attempt to be as compliant as possible in order to allow the body to move as freely as possible. In addition to being an efficient and cost effective actuator, another goal for the actuation system is that it be compliant. Examples of compliant systems include flexures, springs, and other flexible materials. Several strategies were analyzed for this application, but ultimately, a cam and a series of linkages and flexures was chosen for this thesis.

1.1.2 Generation of a moment within a compliant material

One technique used to generate a moment within a compliant-bodied robot is to embed a rigid plate within the soft material (typically silicone, rubber, or a combination of materials). In the fish example that we are focussing on for this thesis, the plate is embedded near the intersection of the tail with the body. Figure 1-2 demonstrates the approximate location where the moment should be generated.

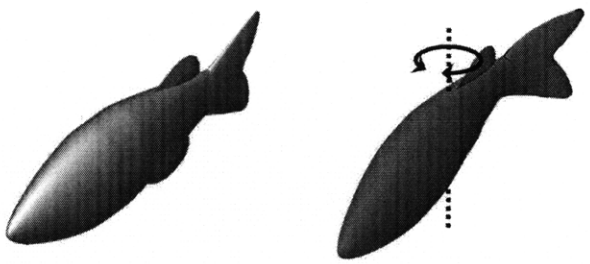

Figure 1-2: The above drawings demonstrate the location of the moment which is generated within the compliant bodied fish. While a fish serves as the example, the principle can be used is other compliant bodied systems (Figure adapted with permission of [3]).

By rotating the embedded plate with cables or rods attached to a motor, a moment is generated close to the fish's tail. This moment forces the soft material to compress on one side of the tail and to stretch on the other side. The material naturally tries to return to an equilibrium stress state, which causes the tail to move to the left or right in order to balance the stress. The motor rotates the plate in the opposite direction to start movement to the opposite side. The process repeats, the plate rotates back and forth, and locomotion is generated as the waves move through the body of the fish to the tail. Typical values for the frequency of the tail section range between two to six Hz or less, which is similar to real fish [3].

1.1.3 New design for moment generation

In the actuation design developed within this thesis, a DC motor rotates in a single continuous direction. In previous designs, motors driving the mechanisms were set to oscillate [3]. The rotation of the motor is transferred into torque through a gearbox which outputs the torque to a cam. As the cam rotates, one side is eccentric and pushes on rods positioned to the left and the right of the cam. These rods contact the cam with a rounded tip so that there is as little friction between the cam and the rods as possible. These two rods can be made of a variety of strong, low-friction materials and, through a system of flexures and joints, pull on a plate, which is embedded in

to propel the fish forward. A picture of the system is provided in Figure 1-3.

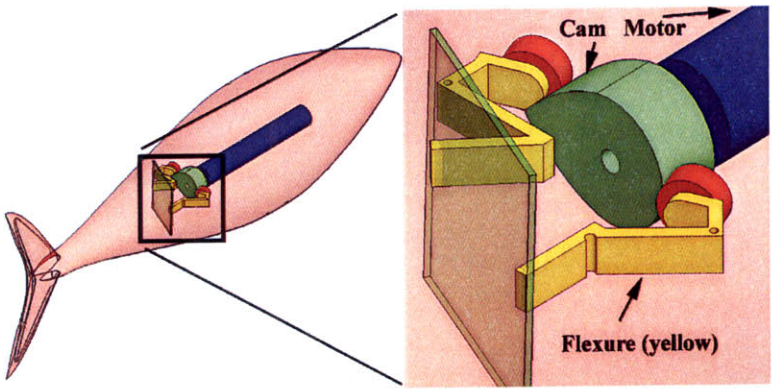

Figure 1-3: These assembly drawings give a visual representation of the actuation design proposed in this thesis. As the cam rotates, the yellow flexures pull back and forth axially along the compliant body.

1.2 Objectives and scope of thesis

In this thesis, I will develop and test a novel actuation system designed for a compliant-bodied fish. This system will propel the fish forward through water using the vibrational waves moving through the compliant body and tail. The target frequency of tail movement will be up to six Hertz (similar to most fish) and the size and weight of the motor and gearbox are minimized to be under two cubic inches and close to neutrally buoyant. While this thesis applies directly to a biomimetic polyurethane fish, it is hoped that a similar design could be utilized without significant modification in other biomimetic or non-biomimetic systems requiring two dimensional, repetitive motion. Examples of some other potential biomimetic applications include other aquatic life (rays or invertebrates), reptiles (snakes and lizards), birds (for the wings), or insects. Within this thesis, I will examine notable previous attempts at using compliant systems for locomotion and the characteristics of fish movement and their implications for design. In addition, this thesis proposes a new flexible actuation system for fish locomotion and discusses the merits and presents experimental modeling of this prototype design.

Chapter 2

Background

Understanding how fish use their bodies to move through a liquid is an important aspect of determining how to mimic their movements. Fish have had many millions of years to perfect their natural swimming abilities, and they are exceptionally adept at moving through water. Imitating this natural ability involves a complex interplay of both mechanical systems and controls. Over the years, researchers have attempted to mimic different types of fish. This has resulted in several different ideas of how to create an artificially swimming fish. Techniques vary in both the structural characteristics of the designs and in the actuation strategies employed. Instead of tackling the whole fish, this thesis focuses on a solution to robotic tail actuation with the hope that the actuator can be utilized in other applications with minimal modification.

2.1 Previous biomimetic systems

The concept of biomimetic systems is not a new idea. There have been many attempts at biomimetic systems dating back for decades. These attempts have included MIT's Robotuna I [6], Festo's Aquaray [7], and Stanford's robotic geckos and cockroaches [8]. While the major principles of robotic design have not changed, the materials and the actuation concepts utilized in the systems have been the main areas of innovation. New advances in materials technology allow for designs to utilize shape memory and piezoelectric materials in addition to the more traditional electric motor and

pneumatic systems. Robotic systems have also become less rigid and more compliant in an effort to be capable of working well within in a wide range of conditions and tolerances. In order to understand how best to effectively mimic a fish, it is important to understand the dynamics of how a fish swims.

2.1.1 Fish characteristics

Fish have the ability to turn in less than a body length, and from a standing start, fish can accelerate rapidly using only a few flicks of their tails at levels of more than 10 g's [9]. Locomotion in fishes is accomplished through a sequential system of smaller muscles which contract in a wave along the fish's body. Once they begin to move, fish utilize their sensory system to detect vortices created by their tails and "push off" of the vortices which allows them to be very efficient swimmers. This ability to take advantage of sensory feedback allows them to avoid obstacles, make quick maneuvers, and become as agile as possible in the underwater environment [9].

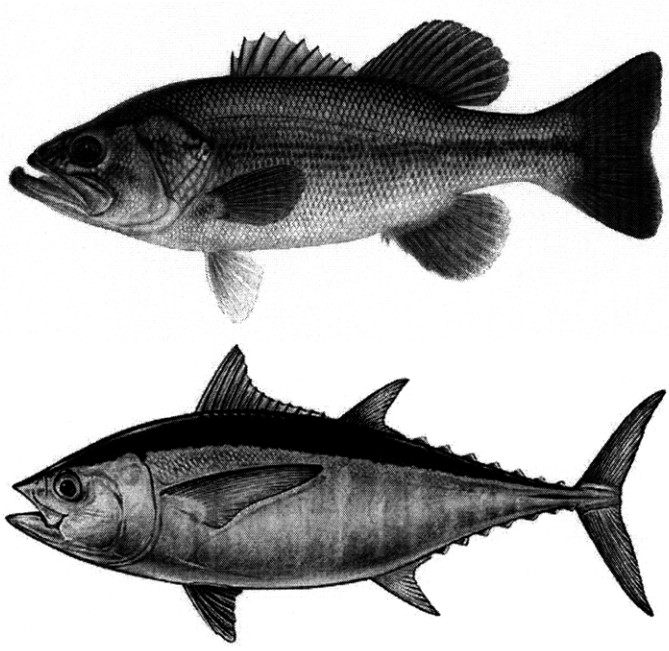

Figure 2-1: Side profiles of Caranguiform and Thunniform fish. A Largemouth Bass (top) represents the caranguiform profile while a Blackfin Tuna (bottom) represent the typical Thunniform profile [10] [11].

In addition, fish have developed different shapes and body geometry in order to

swim efficiently. Two of the most common types of fish bodies are caranguiform, of which the freshwater largemouth bass is one example, and thunniform, of which the tuna is an example. These two body types are not extremely different, and both are efficient swimmers. The difference resides mostly in the body taper to the tail fin and in the geometry of the cadual fins. These two forms are used as examples in Pablo Valdivia y Alvarado's work [3], which provides a foundation and an application for this thesis.

Parameters for actuation

Because we seek to mimic the natural ability of a fish to swim in a straight line and are focusing only on its tail, it is important to clearly define how the natural characteristics of fish will define certain parameters for the actuation system. The following parameters apply to a fish that is 0.3 meters long and made of polyurethane. The frequency of the actuated tail needs to range between two and six Hz. This frequency is similar to a naturally swimming fish and allows the system to produce an optimal amount of thrust. From experimental data collected from Valdivia y Alvarado's previous work, a polyurethane fish that is .3 meters in length generates the highest thrust at about 3.5 Hz and is most efficient at slightly less than three Hz [3]. In addition, the volume of the motor and associated gear train should be less than $2.5in^3$. This size has been selected because the motor must fit within the body, have enough room for mechanisms to attach, and also be light weight so that a large air cavity is not needed to preserve buoyancy [3]. The primary consideration in determining the volume is weight, since the preservation of buoyancy is important to the success of a freely swimming fish. Finally, the Young's Modulus (E) of the polyurethane material is 48624 N/m^2 and requires about 1.4 Nm of torque in order to create a suitable moment for locomotion. This torque must occur near the base of the tail and move in a wave to the tail's end. This system provides only for straight line motion, and does not look into the requirements for changing direction.

2.1.2 Robotuna I

In the mid 1990s, MIT researchers in the Department of Ocean Engineering developed Charlie I, or robotuna. Robotuna used several sets of motors, pulleys, and cables to move the tail of a fish-like robot and generate movement. Robotuna featured a tuna-like profile, and was one of the earlier and more successful attempts at creating a robotic fish. Ultimately, robotuna determined that the flow of water along a moving body can be tuned to enhance swimming characteristics. Robotuna moved in a straight line and needed a harness to keep from sinking. The dynamics behind free swimming fish are very complicated, but the results from robotuna allowed the parameters affecting efficiency and drag to be obtained [9]. Of particular interest to this thesis is the wavelength and amplitude of the body waves. These two parameters are important for tuning the frequency and amplitude of the wave generated by the actuator system.

Support structures

Structurally, robotuna contains a segmented backbone beneath the skin. This structure is composed of eight rigid vertebra with ball bearings at the joints to reduce friction. All other assemblies are mounted to this backbone and the curvature of the fish is created by the angles at which the individual vertebrae meet each other. The outer skin of the robot is flexible and is supported by a series of flexible springs that allow the skin to move and shift with the body. These ribs bend and move to provide support to the outer skin, just as in a real fish.

Actuation techniques

Within robotuna, there are 6 DC motors. These motors are mounted above the water line outside of the body (robotuna is not watertight), and these motors actuate the eight vertebra making up robotuna's spine. The motors use an elaborate system of pulleys and cables to reproduce the tuna's natural muscle structure. Figure 2-2 shows a close up view of the motors, pulleys, and cables.

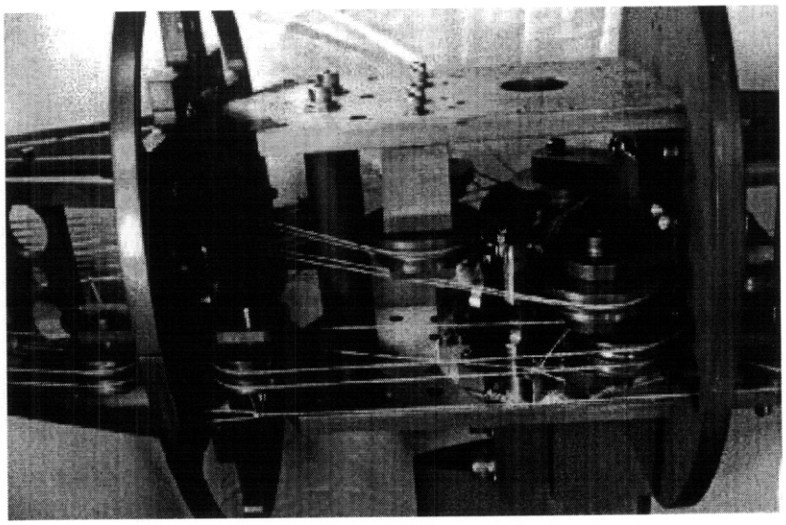

Figure 2-2: Close up view of the actuation system within the robotuna. The complex system of motors, cables, and pulleys can be seen [5].

2.1.3 Festo's Aquaray

The Aquaray was built by Festo, a mechatronics manufacturing company, in order to demonstrate some of the new components and features currently in production at the company. The Aquaray is designed to take advantage of the natural gliding ability of a manta ray through water and reduce the power consumption by flapping its wings and then gliding along through the water. Because it can glide, the Aquaray experiences a natural increase in its range without a corresponding increase in its power requirements [7].

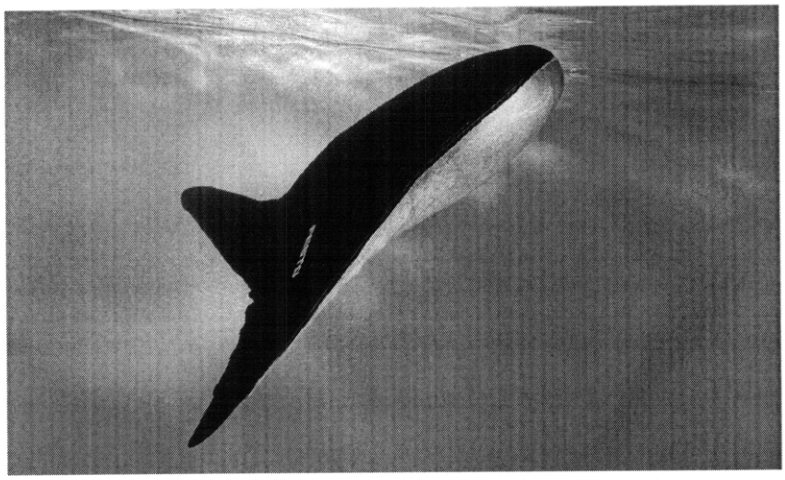

Figure 2-3: The Festo Aquaray. The Aquaray imitates the swimming dynamics of a manta ray [7].

Support structures

The Aquaray uses a system of stiff rods that flex and allow the force to be evenly distributed across the wing. These flexures are similar to the bony rods in a fish's fin. In addition, the 3D deformable skin allows the Aquaray to flex without wrinkling in a variety of directions. Figure 2-4 illustrates the internal structure beneath the skin.

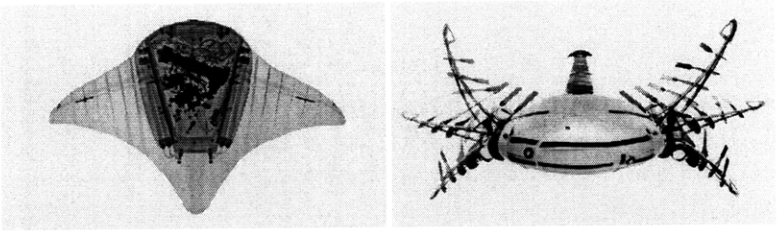

Figure 2-4: The Aquaray's fin flexures allow it to evenly distribute forces across the wings. This makes the Aquaray's movements efficient and imitates the natural model [7].

Actuation techniques

The Aquaray uses a water-hydraulic drive systems and Festo's propreitary fluidic muscles (hollow elastomer tubes made of flexible fibers). These tubes expand in diameter and contract longitudinally when filled with air or water. The contraction allows a smooth, muscle-like movement [7].

2.1.4 Stanford's biomimetic robots

As a Doctoral student at Stanford University, Sangbae Kim [8] created several biomimetic robots that utilize compliant structures in order to climb walls and move. These robots include a gecko, a six-legged wall climbing robot, and a cockroach. The gecko ('Stickybot') uses a compliant foot to climb smooth structures such as glass, white boards, or other smooth surfaces. The wall-climbing robot ('Spinybot') uses small hair-like fibers to cling to the wall and has a compliant foot-like pad that allows it to both cling and release in order to climb. The cockroach ('iSprawl') runs over rough surfaces and moves very quickly at more than 15 body lengths/second.

Support structures

Kim uses plastic or compliant materials in his robot designs. This is seen most apparently in Stickybot which uses a flexible foot to cling to smooth surfaces, and can also be seen in Spinybot's flexible system for assuring that the spines can align and cling properly to walls. Both systems also use a flexible body.

Actuation techniques

Kim's robots use servo motors, DC motors, and pneumatic systems to move the arms and linkages for his robots. His iSprawl uses a pneumatic system to pump air or water through tubes. As the air or water moves through the tubes, it pushes or pulls a wire, which is the leg of the robot. A push/pull wire transmission is also use with the Stickybot, but in this case, the wires are moved directly by the motor [8].

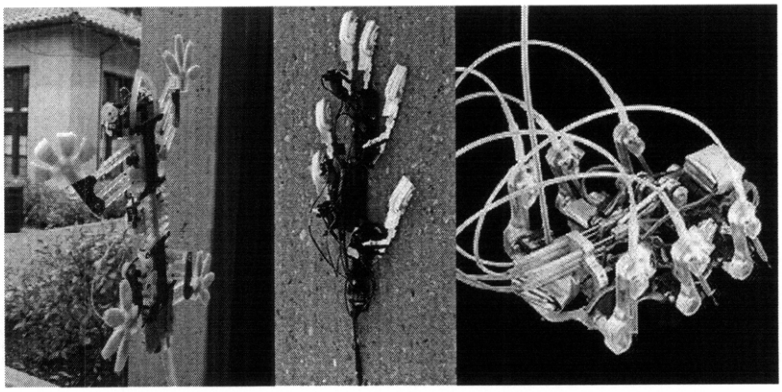

Figure 2-5: Sangbae Kim's biomimetic robots are shown above. They utilize compliant structures and actuators to achieve their targeted motions. Stickybot's feet are compliant, Spinybot's feet are also compliant, and iSprawl utilizes a compliant pneumatic actuation system [8].

2.2 Actuation systems

The chosen actuation system should be inexpensive and relatively simple in comparison to something like the complex robotuna. It is also limited in size and power consumption, since all elements must fit within the robot fish's compliant body. In addition, the system should try to interfere as little as possible with the motion of

the body. The system should be compliant where possible, so that it interferes less and so that it can tolerate the wavelike motions of the body. Ideally, the transmission system will be a compliant material.

The examples above included a variety of actuators, and focussed primarily on servo motors, DC motors and pneumatic or wire transmission systems. In addition to these technologies, new advances in materials have led to several other possibilities.

2.2.1 Muscle-like acuators

Electro-active polymers (EAPs) hold some potential for this application, especially since they can be placed into compact areas. There are two types of EAPs, electronically activated and ionically activated [12]. Electric EAPs use electricity whereas ionic EAPs utilize chemical gradients and electricity in order to create a displacement. However, ionic EAPs are not the fastest way to actuate a system, so they may struggle to function at frequencies of two to six Hz. In addition, electric EAPs require voltages greater than 100 volts and are not the most efficient type of actuator for the amount of displacement that they generate [12].

Table 2.1: Lists the main advantages and disadvantages of conducting polymer-based actuators

Conducting Polymers [13]		
Basic Actuating Material	Advantages	Disadvantages
SMA - shape memory alloy	Individual link control	Difficulty manufacturing
	Multi-functional with high power to weight ratio	High cost, high current
	High bending angle	Temperature based with heat generation
SMP - shape memory polymer	Various transition temperature	Low recovery force
	Large deformation, low cost	Temperature based, slow response
Ionic polymer metal composite	High bending angle	Low force, aqueous environment
Dielectric Elastomer	High strain	High voltage

EAPs currently suffer from low conversion efficiency, a lack of robustness, and a lack of commercially available products [12]. The most commonly available muscle-like systems include piezoelectric actuators (which generate a wave from the displacement of multiple small fibers to move the shaft of the motor) or nickel-titanium wire (NiTi) which has to be heated in order to contract. The problem with the piezoelectric actuators is their cost (greater than 1000 dollars) and relatively small displacement, as they are often utilized for nano-positioning. NiTi wire loses efficiency since it must convert power into heat, and cannot maintain the required frequency since it must contract and then cool two to six times per second.

2.2.2 Voice coil actuators

Voice coil actuators are magnetic motors that can provide linear or rotational actuation. They are called voice coil actuators because their most common use is as a driver for audio speakers. In addition to serving as a driver for speakers, voice coil motors are capable of highly accurate tasks including nano-positioning. While they are efficient, magnetic actuators tend to push with less force as their displacement increases. As such, they lose efficiency at large displacements. In addition, magnetic actuators are typically heavy for their size because of the the coils of wire used inside to generate the magnetic field [14].

2.2.3 DC motors

DC motors are electromechanical actuators with a series of coils used to create a magnetic field and convert a voltage potential into a torque and an angular velocity. They can have brushes or be brushless, and typically have efficiencies somewhere around 65 to 85 percent [15]. Both servo motors and DC motors provide sufficient amounts of power and they are both quick enough to provide motion at the necessary frequency. While there is certainly no perfect actuator, for this thesis, attention is given primarily to DC motors as they represent a commercially well-developed, capable, relatively cheap, and efficient means of actuation. Table 2.2 lists current

technologies and their energy densities under a set of estimated parameter values (material-dependent values are not estimated). While DC motors have the lowest energy density, they are the most practical for this application due to their availability until further advances in materials are made.

Table 2.2: Comparison of Energy Densities of Selected Actuators

Comparison of Energy Densities				
Actuation	Max. energy density	Physical and material parameters	Estimated parameter values	Order (J/cm^3)
Electrostatic	$\frac{1}{2}\varepsilon_0 E^2$	E = electric field ε_0 = dielectric permittivity	$5\ V/\mu m$	~ 0.1
Thermal	$\frac{1}{2}Y(\alpha\Delta T^2)$	α=coefficient of expansion ΔT=temperature rise Y=Young's modulus	$3x10^{-6}C^{-1}$ 100C 100GPa	~ 5
Magnetic	$\frac{1}{2}\frac{B^2}{\mu_0}$	B=magnetic field μ_0=magnetic permeability	0.1T	~ 4
Piezoelectric	$\frac{1}{2}Y(d_{33}E)^2$	E=electric field Y=Young's modulus d_{33} = piezoelectric constant	$30V/\mu m$ 100GPa $2x10^{-12}C/N$	~ 0.2
Shape-memory alloy		Critical temperature		~ 10

2.3 Summary

In this section, the characteristics of fish were covered and the necessary parameters for an actuator were established. In addition, several notable past examples of biomimetic systems were discussed along with their merits. Robotuna led to several important discoveries concerning robotic fish design. Aquaray demonstrates potential uses for newer technologies and actuation systems, and Stanford's Kim has

developed several unique designs using compliant systems and electromechanical actuation. While there are many different actuation systems, each has a different set of strengths and weaknesses, and ultimately, a traditional electromechanical actuator has the best potential for this application due to its relative low cost, adequate power, and speed.

Chapter 3

Actuator design

The actuation system proposed in this thesis consists of a DC motor coupled to a cam, which moves two followers connected to two transmission linkages (flexures) of identical geometry. The whole system is embedded within a cavity inside of a compliant fish body, and the flexures pull axially on a rigid plate embedded in the rear of the fish's body to create a moment near the tail. This moment generates a wave throughout the body, which propagates to the tail and creates locomotion. The DC motor's actuation system has many merits over a servo motor, including greater efficiency, its relative low cost, its scalability, and the fact that it is compliant and will interfere minimally with the body's motion.

3.1 Initial concepts

Several designs were considered in the development of the DC motor and cam actuator. Figure 3-1 shows a design with a vertical motor. The design used gears in order to create a horizontal motion with a yoke and a pin on the surface of a gear. The deflection of the pin in this case depends solely, on the size of the gear. Gears, however, are not compliant and do not mesh well unless properly constrained. A compliant body is not an ideal place to properly constrain gears, and as such, the design was abandoned. The gears could have been replaced with a belt and pulleys, but the belt must be in constant tension, which is also difficult to achieve in a compliant body

because the body will move. The only way around such problems is to build a stiff box for housing the transmission systems, but such a box would inhibit the wave-like motion of the body. As a result, this option was not pursued.

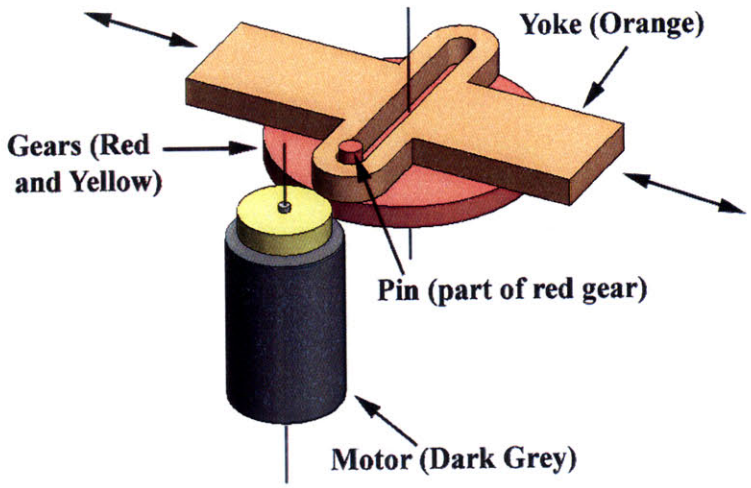

Figure 3-1: This transmission system creates cyclical lateral motion, but also would be hard to constrain within a compliant body. Because of the difficulty of finding adequate constraints, the design was abandoned in favor of finding something more compliant.

Before the cam and flexure system was developed, another design using an oblong cam was considered.(Figure 3-2) This design featured flexible arms and attached to the cam via a ball bearing. This created motion in both the x and y laterally and axially along the fishes body. The cam is rigidly attached to the motor axle, and as the axle spins, the cam rotates along with it. To get an idea of how the system would move, consider this example: in Figure 3-2, the axle is rotating in the direction of the arrow next to it. The axle connects to the cam 5mm from the center of the cam. Because of this off-center location, as the cam continues to rotate 90 degrees in the direction of the arrow, the entire green flexure system will move -5mm axially. Rotating another 90 degrees, the flexure system moves 5mm laterally and returns to its original position in the axial direction. This cycle continues as the cam rotates. Essentially, the flexure system moves in a circle with a 5mm radius. The waves created were to propagate through the flexures to the tail and create a wave in the

tail. However, it soon became clear that rather than move the flexures, this design would most likely oscillate near the motor, but remain idle near the tail because the ball bearing allows the flexures' tips to remain relatively still. This design was not pursued, but it did contain several features that helped guide the development of the final design including the use of a cam, a ball bearing, and a flexure.

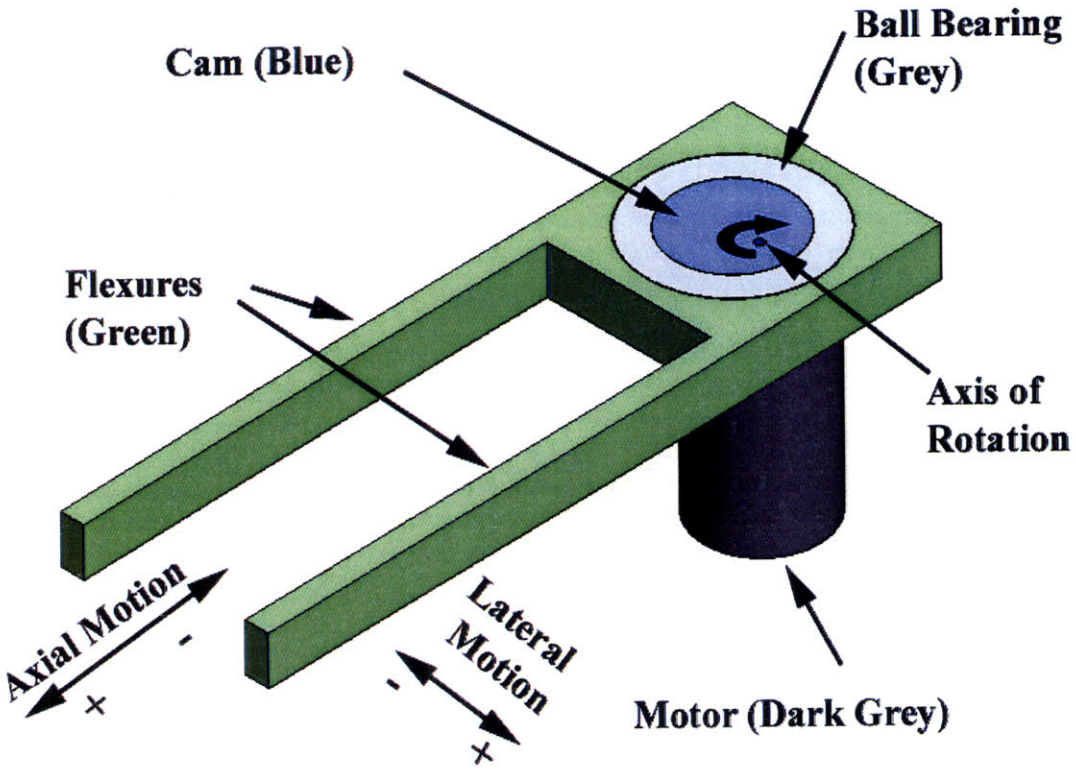

Figure 3-2: Although this design was not pursued, it contained elements that were included in the final design.

3.2 DC motor and cam

In this thesis, a brushless Maxon DC motor coupled to a Maxon gearbox [16] and a linkage transmission will be the primary focus for analysis of the actuator. The entire actuation system is depicted in Figure 3-3. The motor is in shown in blue, the cam in green, ball bearing followers are in red, and the linkages making the transmission are in yellow. The arrows in Figure 3-3 indicate the direction of motion. The design rotates the plate, shown in orange, along a vertical axis running through the center

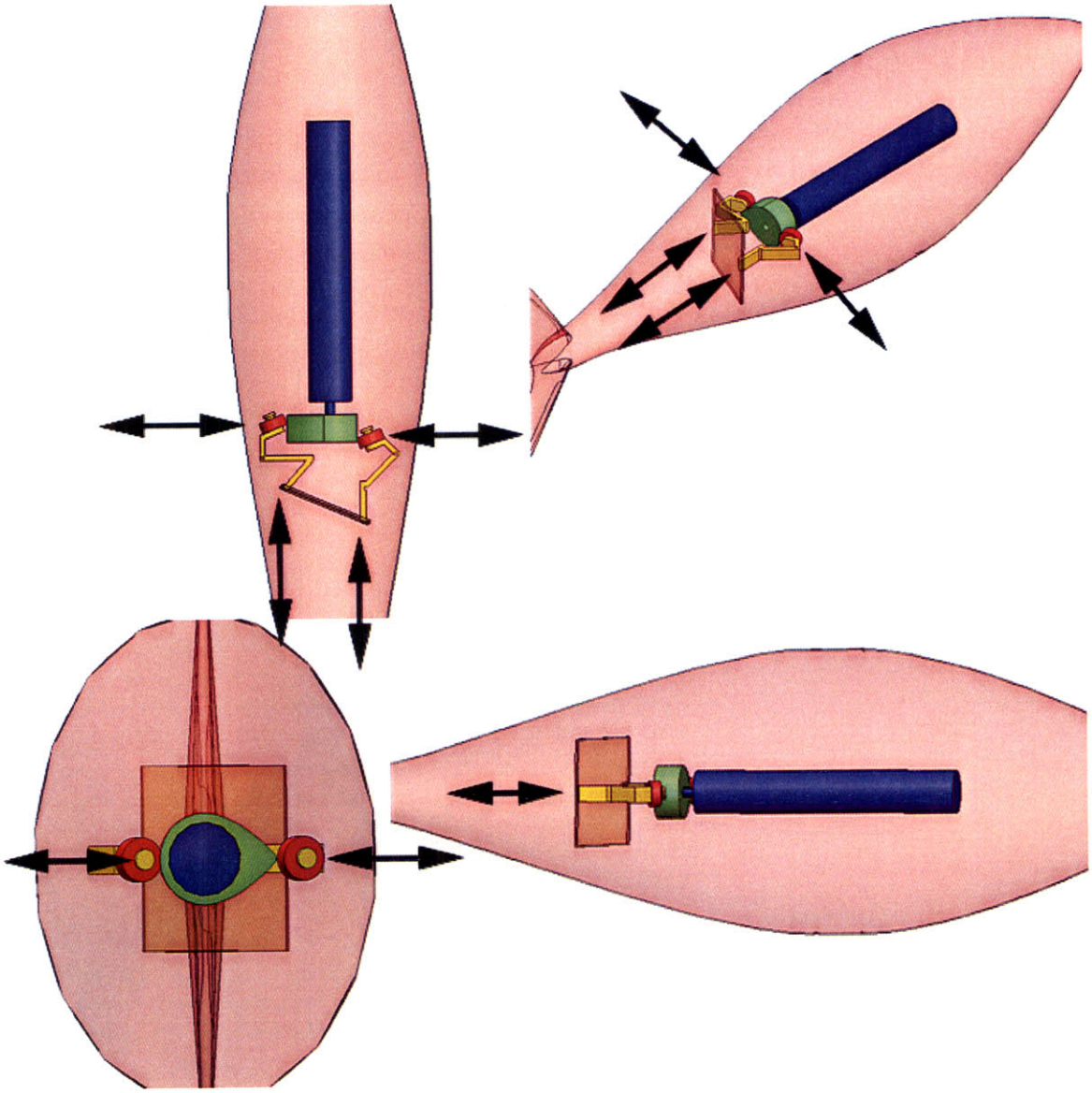

Figure 3-3: The prototype design with a compliant transmission system and a DC motor is shown above in a Top, Trimetric, Front, and Side view. The fish body [3] is a transparent red and the actuator can be seen within.

of the plate. The oscillations of the plate induce a moment in the compliant fish body to generate locomotion. The brushless motor we chose is more efficient than other brushed motors and is a traditional cylindrical shaped DC motor. This is not the only type of motor that could be used. Other motors were considered and could perform equally well including flat motors or linear motors. However, the chosen motor and gearbox provide a good baseline for evaluation of the overall design. All

the different maxon motors and gearboxes considered for the mechanical actuation system are listed in Table 3.1. The table also gives their performance characteristics.

Table 3.1: Motor and Gearbox Specifications

Motor and Gearbox Specifications						
Motor	Gearbox	Gear Ratio	Max Cont. Torque (Nm)	Angular Vel. (RPM)	Volume (in^3)	weight (g)
200142	301171	47:1	2.773	60.85	3.73	312
	266595	32:1	1.888	89.375	3.73	312
	301173	26:1	1.534	110	3.73	312
251601	301173	26:1	2.191	202.31	4.12	334
	301175	18:1	1.517	292.22	4.12	334
232241	143991	231:1	3.210	164.07	1.24	101.7
	143988	128:1	1.779	296	1.16	123
167129	143976	19:1	.7068	1063	2.18	175
226006	166165	66:1	1.537	42.42	2.82	252
200187	134173	231:1	3.000	17	2.65	113

Some motors accept several different types of gearboxes, so their overall output and size can be modified. Motors such as the maxon 251601 are wide and flat instead of long and cylindrical. In addition to differences in size, the orientation of the motor within the fish body can be changed in order to accommodate different lengths. The flat motors can be placed vertically within the fish, and thus have less of an impact on the wave traveling through the fish body. Although they are longer than flat motors and must be placed axially within the body, cylindrical motors have a lower overall volume, which is important for adding other pieces of equipment inside the body. Two different motor positions and orientations are shown in Figure 3-4. In addition to the DC motor, a linear actuator could create a motion similar to the cam. DC motor suppliers other than Maxon could be used.

The angular velocity of the motor shaft is used to turn an oblong cam show in Figure 3-5. One half of the cam maintains a radius of 10mm, and the other half increases from 10mm to a maximum radius of 15mm, and then back to 10mm. This 5mm eccentricity is what moves the followers and flexures to create motion. The size

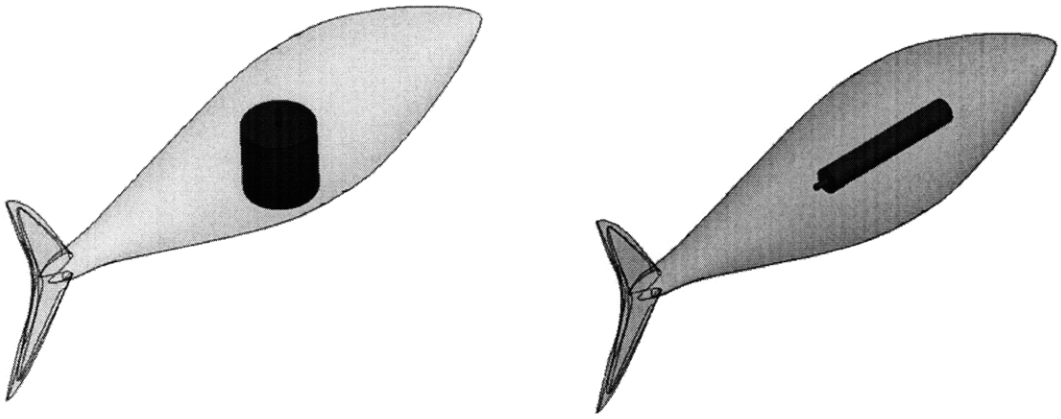

Figure 3-4: Maxon makes both flat motors and cylindrical DC motors. Other types of motors are also compatible with this design, since the transmission system works with different types and sizes.

and geometry of the eccentricity is important in that it cannot be too large or too steep. If the eccentric region of the cam becomes too large or increases to its maximum radius too quickly, it will bend the follower rather than provide the desired horizontal push. Friction between the cam and the follower should be kept at a minimum so that the follower does not require the motor to output higher levels of torque. For the purposes of this thesis, an eccentricity of 5mm was chosen.

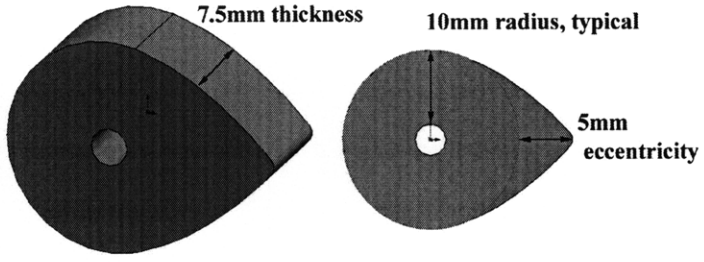

Figure 3-5: This view shows the dimensions of the cam and how there is a maximum of 5mm of eccentricity. The gradual increase to 5mm takes place along half of the outer edge of the cam. The other half remains at a radius of 10mm.

3.3 Follower and flexure system

The follower and flexure system represents the transmission system within the fish body. The followers are ball bearings (red in Figure 3-3) and the flexure system can be made of a variety of materials (yellow in Figure 3-3). This transmission can be scaled and the lengths of the flexures can be modified in order to suit different motors and motor sizes. While part of the follower system is compliant such that the angles flex, each flexure has a fixed right angle. At this right angle, the force is transferred from a lateral to an axial force. In addition, at these angles, the flexure is fixed in space by a pin joint. The joint maintains the same distance from the motor via means of two brackets above and below the joint. In Figure 3-6, only one bracket is shown in the left and center drawings for clarity. These brackets are fixed to the motor so that they do not change the distance between the motor and the joints. As the linkages pivot on the fixed pins, they transfer force from the cam, to the embedded plate. It is important to note that the linkages pull on the embedded plate rather than push on it. The transmission flexures are located within a cavity inside the fish body so that they can move freely. They are partially embedded at the ends where they join to the embedded plate. The silicone rubber acts as a spring that pushes against the flexures, which in turn keep the follower in contact with the cam. The follower is a ball bearing attached to the linkage transmission. One potential challenge in this design is that the friction changes as the linkage rotates about the fixed pin. This rotation affects the red ball bearings' contact angle with the cam, which in turn changes the friction.

3.4 Summary

The actuator design was outlined in this chapter. Its advantages include that it has compliant structures and scalability. The dimensions and characteristics of the motor and gearbox can be changed in order to accommodate different sizes and shapes of fish. In addition, the size of flexures can be modified to produce different torques and displacements depending on the size of the fish body. The easiest way to scale

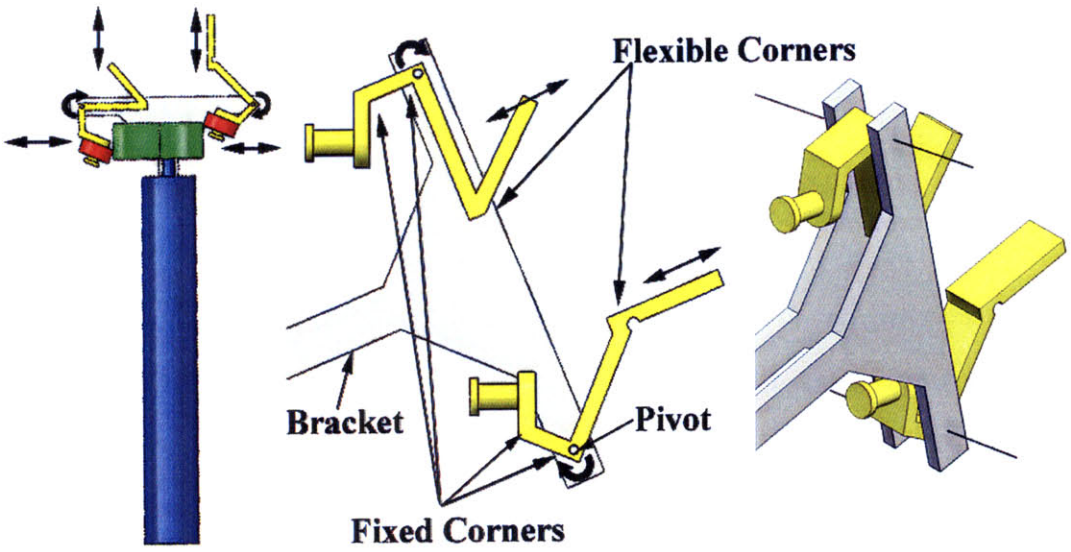

Figure 3-6: The brackets which support the flexures are shown in this drawing. The bracket clamps to the motor. Also, there should be a bracket on the top and bottom of the flexures as shown in the upper left.

the system is use the fish body length as a scaling factor. It includes an eccentric cam that pushes on two flexures alternatively and these flexures, in turn, pull on an embedded plate in the fish's tail. Other designs were analyzed and subsequently rejected due to lack of compliance of because of their size or resulting motion.

Chapter 4

Actuator Model

In order to evaluate the effectiveness of the proposed mechanism before it is built, a mathematical model was created for the actuation system outlined in Chapter 3. The model makes several assumptions, and can be modified such to accommodate biomimetic structures of a different size and stiffness. The flexures can be made of a variety of materials or 3D printed, so their stiffness and mechanical properties can be modified by changing the materials used for them. Different link ratios can achieve different end forces and torques, and the system as a whole is shown to be viable by the model.

4.1 Model parameters

In order to discuss the model, first the variables and associated structures should be defined. Figure 4-1 displays the model variables. There are two pinned joints on the linkages. These are pinned by a bracket attached to the motor, which keeps their distance from the motor relatively constant. In addition, these joints are fixed in space and remain at a right angle, but a pin provides an axis for them to rotate about. a will be partially embedded in the polyurethane, while the rest of the transmission system will be housed in a cavity within the fish body. a will attach to an embedded plate and the polyurethane will serve as a spring that will push the followers against the cam. Each linkage is labeled sequentially. In addition, the angles created by the

linkages are also labeled. The linkages have flexural joints between a and b. The fixed joints between d and c are fixed at 112.5 degrees and the fixed joints between a and b are right angles.

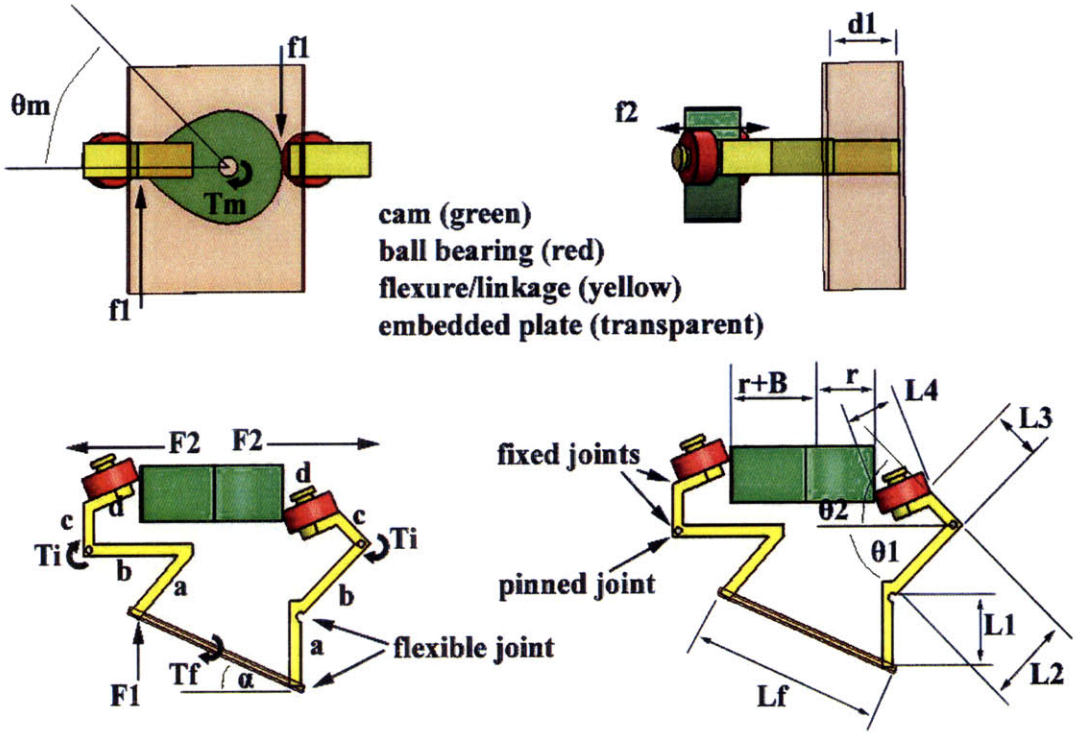

Figure 4-1: Model variables.

4.2 Actuator dynamics

The purpose of actuation is to generate a moment, T_f, that creates a vibrational wave that propagates through the soft body. The compliant fish exploits these waves to move forward [3]. Because a moment creates the waves, identifying the torque necessary to create the moment is important. The torque at the embedded plate is denoted T_f and the lever arm is half the length of the plate, which is denoted L_f. The formula for T_f is found in (4.1).

$$F_1 = \frac{T_f}{(.5 \times L_f)} \tag{4.1}$$

In this equation, the resulting force, F_1, is the force transferred through a to b.

After finding F_1, the next step is to convert F_1 into a torque. This torque is an intermediate torque that acts about the pinned, right angle joints in the flexures and is denoted as (T_i) in (4.2). This intermediate torque is transferred through the rotation of the joint from b to c. One of the more interesting aspects of this torque is that it varies based on the angle of b with the horizon as shown in Figure 4-1. This changing angle is θ_1 and is given in radians.

$$T_i = (F_1) \times L_2 \times \cos\theta_1 \tag{4.2}$$

The next step is to transfer T_i into a force. This second force, F_2, is the force that is exerted through c and d to the surface of the cam. The equation for F_2 is defined in (4.4). This force is the normal force between the cam and the follower. The angle of c is θ_2, and it varies directly with θ_1 as shown in (4.3) and is in radians.

$$\theta_2 = (\frac{\pi}{2} - \theta_1) \tag{4.3}$$

$$F_2 = \frac{T_i}{(L_3 \times \sin(\theta_2))} \tag{4.4}$$

After having obtained F_2, this force can be used to obtain the amount of torque necessary from the motor to turn the cam. This motor torque is denoted T_m, and it is defined in (4.8). The coefficient of friction of the ball bearing follower is μ_1 and it ranges from .001 to .020 depending on lubrication and other factors [17]. The overall value of the friction force resisting the rolling of the ball bearing and the motion of the motor is f_1 [18]. In addition to the rolling friction, there is sliding friction of the bearing across the surface of the cam denoted f_2 [18] with coefficient of friction of mu_2. The typical radius of the cam is 10mm, and is represented in (4.8) by the variable r, which is defined in (4.7). The maximum eccentric radius of the cam is 15mm and is represented by B. The eccentricity varies as an inverted sine wave as at any point in time, one of the two followers is being pushed requiring a greater motor torque. This variability with position is represented by θ_m, the angular position of the maximum radius of the cam in radians.

$$f_1 = \mu_1 F_2 \tag{4.5}$$

$$f_2 = \mu_2 F_2 \tag{4.6}$$

$$r = R + B \times |(\cos(\theta_m))| \tag{4.7}$$

$$T_m = (2(f_1 + f_2)) \times r \tag{4.8}$$

4.3 Constitutive relations

In the last section, the mechanism's torques and forces were obtained. In this section, the focus will be on the application of the equations to created performance modeling formulas for determining how the above parameters and design limitations influence the amount of torque that can be generated with different motors and with different transmissions. The intention of this section is to develop equations which can be plotted in order to model the variety of possibilities that can be obtained from changing variables. This should allow for optimization of the size and speed of the motor and transmission elements in addition to determining the appropriate eccentricity of the cam size.

One of the more interesting aspects of the system is how the length of link 2 and link 3 influence the required motor torque. Motor torques vary across time, but we are interested in the maximum torque and how this torque translates to the embedded plate. The ratio between link 2 and link 3 is given as x and defined in (4.9). (4.10) shows how this ratio and the motor torque (T_m) influence F_1.

$$x = (\frac{L_3}{L_2}) \tag{4.9}$$

$$F_1 = \frac{T_m}{r} \times x \tag{4.10}$$

x is a useful ratio which can be used to roughly calculate torque and displacement in the system. The displacement of the cam has an influence on the end plate's displacement. The desired displacement of the embedded plate, d_1 is roughly the displacement caused by the cam's eccentricity multiplied by the ratio x. (4.13) Similarly, a rough estimate for (T_f) is in (4.11), which is derived from (4.10). In these two instances, x becomes a valuable tool for estimation.

$$T_f = T_m \times x \tag{4.11}$$

In addition to influencing the transfer of motor torque to the force on the embedded plate, F_1, the linkage length ratio also influences deflection, or the length of travel of the linkages and the embedded plate. The displacement of the embedded plate (orange in Figure 4-1) is represented by the variable d_1. Assuming that the cam eccentricity is constant, the length ratio of c over b is directly correlated to the displacement as shown in (4.13). In addition, the length of c is bounded geometrically by the sides of the fish. The length L_3 must be between 7 and 11mm. In addition, the ratio x is bounded between .1 and 3.6. For this size of fish, higher ratios are impractical because the flexures would not be either run into each other or stick out of the fish. The length of d_1 is defined in (4.12) and is influenced by B, the length of the eccentricity of the cam, and by the ratio x.

$$d_1 = Bx \tag{4.12}$$

However, deflection in the system is not so simple. The above model supposes that there is no beam bending or buckling, but this is not the case. Beam bending plays a role because the flexure system is flexible and compliant. (4.13) is the beam bending equation for the angle of deflection, ϕ. In this situation, I is the area polar moment of inertia, which governs the geometric properties of the flexures. E is the Young's Modulus, and P is the force perpendicular to the flexure.

$$\phi = \frac{(P \times (L_2^2))}{(2EI)} \tag{4.13}$$

In order to relate this equation to the torques in the system, the force, P, and the length of a link, L, are placed on one side of the equation, and on the other side, a value is multiplied by the length. This value is simplified to K, which is shown in (4.15) and in the underbrace in (4.14).

$$P \times L = \underbrace{(\frac{2EI}{L})} \times \phi \tag{4.14}$$

$$K = (\frac{2EI}{L}) \tag{4.15}$$

In addition to bending, buckling must also be considered, especially in a. The formula for buckling contains a value denoted K that varies depending on the configuration of a beam's endpoints. In this case, the endpoints are pinned, and K is one. The Young's Modulus, E and the area moment of inertia, I also influence beam bending, as shown in (4.16).

$$F_B = \frac{\pi^2 EI}{(KL_1)^2} \tag{4.16}$$

As an example of how the buckling equation works, if F_B is less than F_1, then a will buckle. Buckling will be influenced strongly by the geometry of a and by utilizing the correct geometry for a, buckling can be eliminated from the final equation.

The total torque on the flexure for an output force of F_1 exerted over L_1 is defined in (4.17).

$$T_i = K\phi - F_2 L_3 \times \sin\theta_2 \tag{4.17}$$

4.4 Performance parameters

The equations in the above section provide a means to calculate the appropriate materials and geometric properties of the actuation system in order to meet certain performance parameters. Based on experimental data collected by Valdivia y Alvarado in his doctoral thesis, the appropriate performance requirements for the two primary types of biomimetic fish that he built are in Table 4.1 [3]. These are the specifications that will be used to analyze results from the models that were developed in the preceding part of Chapter 4.

Table 4.1: Performance Requirements for Compliant Biomimetic Fishes

Performance Parameters			
Fish length(m)	T_f(Nm)	d_1(mm) (about 3 percent of body length)	Frequency(Hz)
0.3	1.4	10 to 15	2.0 to 6.0
0.148	0.1	5 to 10	2.0 to 6.0

Chapter 5

Simulation, Results and Discussion

After defining the mathematical framework for this prototype system, the system performance can be simulated. Using geometric and practical boundaries, variables can be assigned and the optimal solutions and dimensions can be determined. Graphs of the values are based on the Equations at the end of Chapter 4 which model the system (Equation 4.10 through Equation 4.16). The first set of graphs determine the output force and deflection without factoring bending of linkages b and c into the equation. The second set shows the beam bending data for both linkages and the final set factors bending into the entire model. These graphs are useful for determining an appropriate x ratio as well as determining an appropriate flexure material based on the Young's modulus (E). The geometry of the flexures will be important as well since it will affect the moment of inertia (I) for the flexures which in turn influences the amount of bending. In this case, bending is a loss in the efficiency of the system; however, flexures are still attractive as they reduce interference with the body waves propagating through the fish. Several assumptions are built into the model. These assumptions include the following: the length of c must be between .007 and .011mm for our specific model, that the flexures are considered rigid until bending is considered, and that the entire system is massless.

5.1 Simulation

Figure 5-1 illustrates the variation between the motor torque, T_m, and the force, F_1, exerted on the embedded plate. The different lines represent different x ratios ranging from .1 to 3.6. The lowest plot lines (blue and green) represent an x value of 3.6, while the highest plot lines represent an x value of .1. The blue line represents a complete lack of friction, while the green line represents the friction of the ball bearings. The results are very similar due to the bearings' low coefficient of friction. The red line running through the center of the chart is a line that marks the output force, F_1,necessary to generate a proper T_f based on the size of the fish and on the size of the plate. While this plot shows the required torque for a ball-bearing follower, if friction is increased by two orders of magnitude (typical coefficient for some plastics) the motor torque required to get the same F_1 will increase.

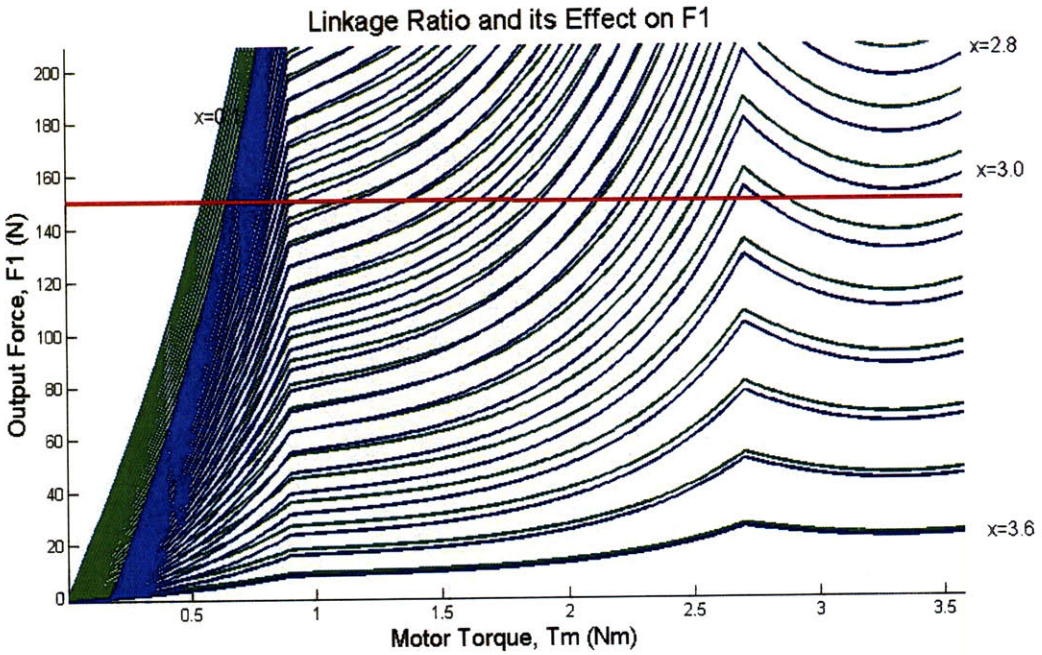

Figure 5-1: The relationship between x, T_m, and F_1.

Qualitatively, the significance of Figure 5-1 is that the graph indicates how the ratio of lengths of the two flexures, b and c, scales the output force, F_1 based on the original motor torque. In addition to scaling the torque, the x ratio also scales the final deflection.

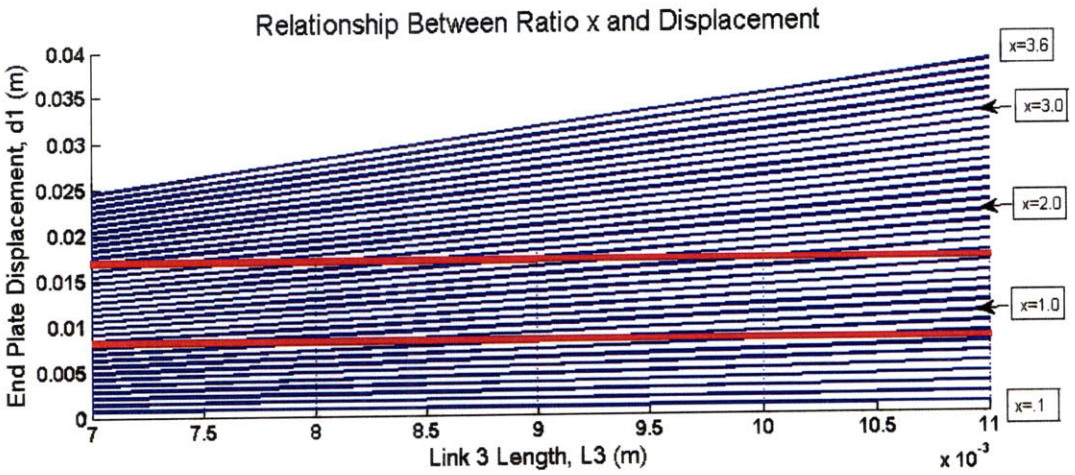

Figure 5-2: Plot 2 illustrates the relationship between x, d_1, and c.

The deflection scales linearly according to Equation 4.12. Figure 5-2 illustrates how the the ratio x influences deflection of the embedded plate. On this plot,the highest plot line (blue) represents a x value of 0.1 and the lowest plot line represents a x value of 3.6. The red lines passing through the center of the graph indicate the upper and lower bounds on the displacement that the actuator needs to achieve at the end plate. In order to be a viable system, the x ratio for a given length of L_3 must not only produce the required amount of torque, but also be able to fulfill the performance requirements as outlined at the end of Chapter 4, such as creating a displacement between 10mm and 15mm.

Another performance requirement was that the frequency of the fish's tail be in a range of two to six Hertz. The proper frequency to generate movement is important and varies slightly with the body profile and material. In Figure 5-3, the frequency is plotted according to the angular velocity of the motor. This is a linear system and the proper range for our application is bounded by the red lines.

From the plot in Figure 5-3, the proper angular velocity of the motor must fall within a range from 120 rpm to 360 rpm. From the work of Valdivia y Alvarado, the most efficient frequency for most of the fish we are using is slightly less than three Hz; however, the highest thrust is obtained at 3.5 Hertz. Three Hertz is 180 rpm while 3.5 Hertz is 210 rpm.

Up until this point, the simulation has considered the flexures in the transmission

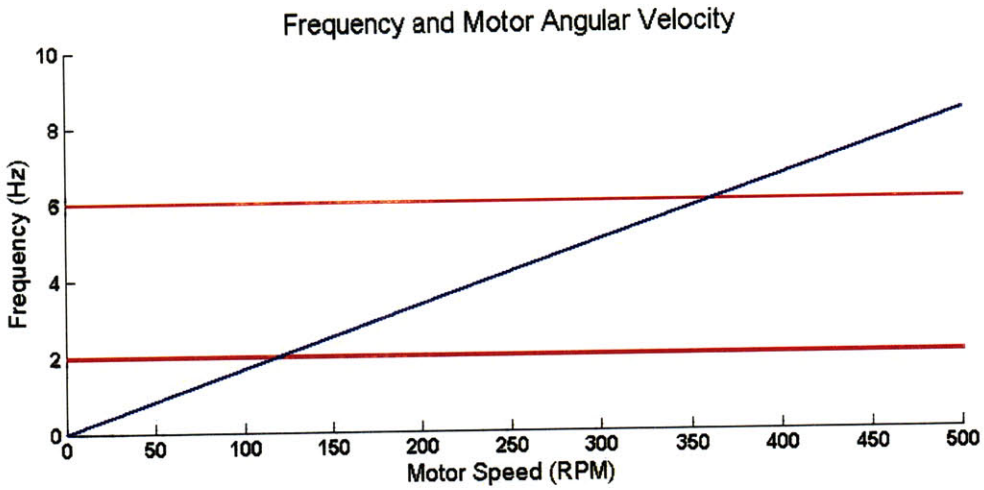

Figure 5-3: The relationship between angular velocity and tail frequency

to be rigid. However, this is no the case, and they are flexible. The amount of deflection and bending in the flexures is dependent on the area moment of inertia (I) and the Young's Modulus (E) of the flexures. Figure 5-4 illustrates how the output force, F_1 decreases as deflection increases.

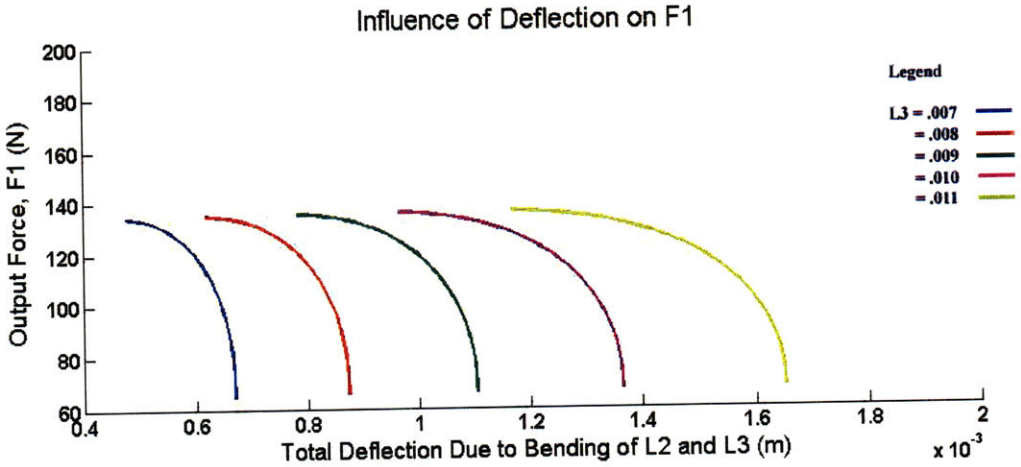

Figure 5-4: The relationship between Force and Beam Bending Deflection

The force and deflection plot should aid in material selection. In addition, losses in F_1 from deflection can be modeled and the parameters E and I can be changed in order to reduce the losses.

5.2 Design Example

The simulations above help to determine which motors, gearboxes, and flexures have appropriate values for the actuator. While many different motors could fit the above specifications, I'll provide a simple example to demonstrate the usefulness of the simulation. Specific values for the system parameters are listed in Table 5.1.

Table 5.1: Example Performance Requirements for Compliant Biomimetic Fishes

Example Parameters			
Fish length(m)	T_f(Nm)	d_1(mm)	Frequency(Hz)
0.3	1.4	10	3.0

The desired torque at the end plate is 1.4Nm. Because the length of the endplate, L_f, is 0.035m, the force, F_1 must be about 150N or greater. The first plot (Figure 5-1) helps determine the optimal ratio of x for a given force and motor torque. There are two peaks for each value of x. Both peaks must be above 150N in order for the flexures to provide enough torque to generate 150N of force for F_1. From following the lines, an x value of 2 is the largest value of x for which 150N of force is generated.

In the second plot (Figure 5-2), the specific lengths of b and c can be determined by finding the correct x line for the value of x determined from plot 1. Follow the x value line into the red region until it intersects with the correct displacement. This is the length of c, L_2. Multiplying L_2 by the ratio gives the length of b, L_2. In this example, L_3 is 7mm. This means that L_2 is 14mm in length.

After obtaining the proper lengths of L_1, L_2, L_3, and L_4, the buckling formula can be applied from Equation 4.14. The geometry can be adjusted to avoid buckling, and for this example, if the flexures are 2mm wide and 6mm tall, a is the only link close to buckling. In this case, the buckling force, 350N, is still twice as high as F_1 and the beam does not buckle, so these dimensions are appropriate.

Once the flexure ratio and appropriate linkage lengths are determined, the torque required of the motor and gearbox can be obtained by multiplying the ratio x by the torque on the endplate T_f. In this case, T_f is roughly 1.4Nm. This example is

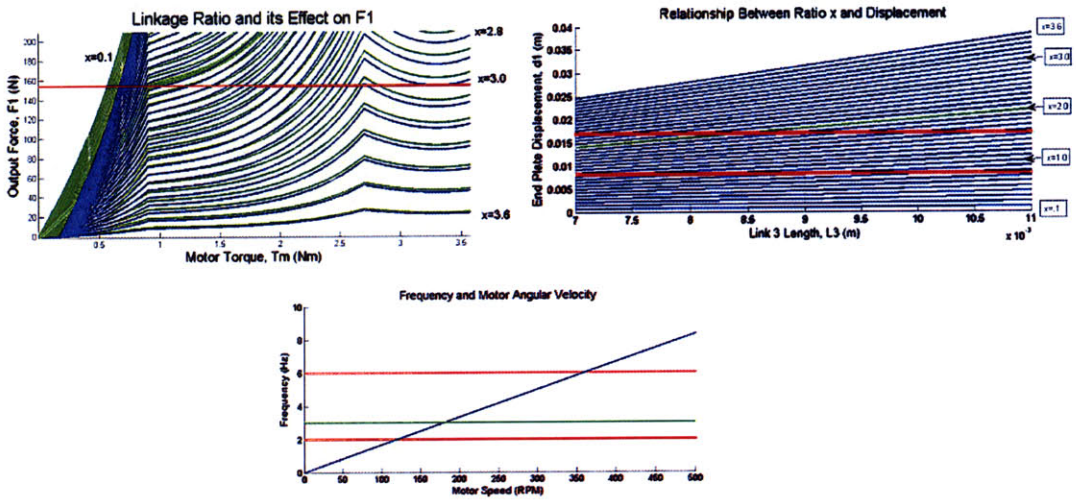

Figure 5-5: The lime green lines indicate the solution for the given parameters in table 5.1. These plot demonstrate how the lines are followed to choose a properly sized motor.

outlined in pictures below in Figure 5-5. The selected lines are in green. Table 3.1 is reproduced below for reference. There is a motor and gearbox combination that fits the rough requirements of our system, at least 2.8Nm (or more for losses based on friction and the deflection from bending in Figure 5-4) of torque and a frequency of about three Hertz. Motor model 232241 and gearbox 143991 provide the correct values.

The simulation as outlined above was verified using rotational matrices and the known geometry of the flexures as outlined above. In addition, the angle of deflection of the embedded plate, α, was calculated from the length of the plate and the x-y coordinates of the plate. These calculations can be referenced in Appendix B. For the simulation above, the matlab code can be referenced in Appendix A.

5.3 Discussion

The simulation above determines the proper motor sizing, lengths of flexures, and can model the effects of changes in different parameters or variables. Ultimately, the size of the motor and transmission are bounded by the limits of geometry, and in

Table 5.2: Motor and Gearbox Specifications

Motor and Gearbox Specifications						
Motor	Gearbox	Gear Ratio	Max Cont. Torque (Nm)	Angular Vel. (RPM)	Volume (in^3)	weight (g)
200142	301171	47:1	2.773	60.85	3.73	312
	266595	32:1	1.888	89.375	3.73	312
	301173	26:1	1.534	110	3.73	312
251601	301173	26:1	2.191	202.31	4.12	334
	301175	18:1	1.517	292.22	4.12	334
232241	143991	231:1	3.210	164.07	1.24	101.7
	143988	128:1	1.779	296	1.16	123
167129	143976	19:1	.7068	1063	2.18	175
226006	166165	66:1	1.537	42.42	2.82	252
200187	134173	231:1	3.000	17	2.65	113

any design, factors such as volume, size, and weight will play important roles in the future development of this system.

In this simulation, the size of the motor determines how much torque is generated. However, this does not have to be the case as a smaller motor with multiple flexures could be utilized. This would have limits, because another property of this system is that the initial eccentricity of the cam determines the end plate displacement after it passes through the transmission, and either increases or decreases in length.

The link between cam eccentricity and the x ratio and their influence on torque and displacement is crucial. These factor influence the selection of a motor and transmission. However, angular velocity seems to be largely separate from being influenced by the x ratio or cam eccentricity.

Deflection is important in the system, and its effects on the output force and displacement should factored in and depend on the flexure material. The final simulation of bending influences the selection of material for the flexures and the flexure geometry. If the correct size and stiffness cannot be found, composite materials with a soft core may be the answer based on the number of life cycles they can tolerate before fatiguing.

Weight is a key factor to consider in the analysis of any potential design. The less an actuator weighs, the less area within the fish needs to be kept empty. As with any free-swimming system, controlling buoyancy is one of the largest challenges. Adding a cavity within the fish body could be one way to compensate. The cavity could be full of any material in order to achieve neutral buoyancy. In addition, weight distribution is also important. Heavy items should be placed low within the fish's "belly" with lighter items or buoyancy cavities should be placed within the upper half of the fish.

Because the transmission system is compliant and because waves are the primary means of power and transmission in this system, it may be possible to use the natural frequency of the flexures in order to generate a larger force by operating the motor at the natural frequency of the entire system. In this way, a larger moment could be generated in the fish tail and large deflections could be obtained without a large initial torque.

Chapter 6

Conclusions

6.1 Thesis contributions

The actuation system outlined in this thesis is the result of research about the different actuation technologies available today. As technology continues to change, other options may present themselves in the future. After weighing all potential technologies, it was determined that a DC motor and compliant transmission would allow the most capability given the requirements for the system. In addition, DC motors and transmissions can be scaled based on the size, shape, and the specific requirements of the application. The model and simulation provided in this thesis is applicable to the development of systems utilizing the actuator. Ultimately, we hope that this actuation system can be utilized in multiple applications and can enhance the viability of these systems.

6.2 Recommendations for future work

The work presented in this thesis suggests the viability of a compliant actuation system for a compliant-bodied fish. Future efforts should focus on the selection of materials and the building and testing of the actuator. Proper material selection is important so that the flexures do not fatigue quickly and so that proper flexibility is maintained. In addition, multiple links could be used to gain different amounts of

torque or displacement. Further research should be given to new types of motors and gearboxes in an effort to reduce the overall size of the system. This actuation system could potentially work in other compliant structures, and efforts should be made to increase the range of robotic systems in which this actuator could be utilized.

Appendix A

Matlab code

```
% Force and Torque

ratio=.1;
Tf=1.4;
lf=.038;
mu1=.30;
l2=(.001:.035);
theta1=(0:45);
l3=(.001:.011);
theta2=(90-theta1);
thetaM=(0:360);
B=.005;
mu2=.06;
R=.01;
r=R+B*abs(cos(0.0174532925.*thetaM));
F1=Tf/(.5*lf);
f1=F1*(mu1);
Ti=(F1+f1)*l2*cos(0.0174532925.*theta1);
```

```
F2=Ti./(l3*sin(0.0174532925.*theta2));
f2=(mu2)*F2(1,1);
Tm=(0:.01:3.6);
hold on
while ratio < 3.6;
    F1=((((Tm)./r)-f2*2)).*(ratio);
    F=((Tm./r)).*ratio
    plot(Tm,F1,Tm,(F))
    ratio=ratio+.1;
end
hold off
```

```
% Linkage Ratio and Displacement

theta1=(0:45);
theta2=(90-theta1);


ratio=.1;
l3=.007:.001:.011;
hold on
while ratio < 3.6;
    l2=l3.*(ratio);
    d1=.005*ratio;
    plot(l3,d1)
    plot(l3,l2)
```

```
    ratio=ratio+.1;
end
hold off
```

```
% Frequency and Angular Velocity

rpm=0
hold on
while rpm < 500;
    H=rpm/60;
    plot(rpm,H)
    rpm=rpm+1;
end
hold off
```

```
% Bending

mu1=.30;

thetaM=(0:360);
```

```
B=.005;
mu2=.0015;
R=.01;
r=R+B*abs(cos(0.0174532925.*thetaM));

f1=F1*mu2;
Ti=(F1+f1)*l2.*cos(0.0174532925.*theta1);
F2=Ti./(l3*sin(0.0174532925.*theta2));
f=mu2*F2(1,1); %f is of negligible size since a ball bearing is used.
Tm=(0:.01:3.6);


b=.006;
h=.003;
E=2*10^9;
density=1100;

bendL2=(P2*(l2^3))/(3*E*I2);
bendL3=(P3*(l3^3))/(3*E*I3);

hold on
l3=(.007);

while l3 < .013;
    Tf=1.4;
    lf=.038;
    F1=Tf/(.5*lf);

    theta1=(0:45);
```

```
    theta2=(90-theta1);
    I3=(b*h^3)/13;
    I2=(b*h^3)/12;
    P2=F1*sin(0.0174532925.*theta2);

    phi1=(P2*(l2^2))/(2*E*I2);
    phi2=(P3*(l3^2))/(2*E*I3);
    K1=(2*E*I2)/l2;
    K2=(2*E*I3)/l3;
    ratio = .1;
    l2=l3*ratio;

    while ratio < 3.6;
        F2=(F1*l2*cos(0.0174532925.*theta2))/l3;
        P3=F2.*sin(0.0174532925.*theta2);
        T1=((K1*phi1))+(F1*l2.*cos(0.0174532925.*theta2));
        T=(K2*phi2)+T1;
        F=T/l2;
        deflection=(phi1);
        plot(deflection,F)
        ratio=ratio+.1;
    end
    l3=l3+.001;
end
hold off
```

```
% Appendix B code
```

```
theta_t=(45*0.0174532925);
x_t=(0:5);
d=7;
c=7;
b=14;
a=15;
L_f=35;
x=9.89;
y=9.89;
i=4.94;
j=4.94;
A=[cos(theta_t),sin(theta_t);(-sin(theta_t)),cos(theta_t)];
B=[x;y];
C=[i;-j];
A*B
A*C
alpha=asin(10/(L_f))
```

Appendix B

Alternative modeling method

An alternative method to verify the displacement results obtained from the equations includes using rotational matrices in order to assure that the system performs as predicted. The only part of the linkage system that rotates is the pinned joint. This pin serves as the origin about which the links b and c rotate. First, the coordinates of the joint between b and a and the joint between c and d must be determined. Because b and c are 45 degrees (θ) above and below horizontal, using simple trigonometry, we can determine the initial starting coordinates. Because the angle is 45 degrees, the x and y coordinates of the endpoints of the linkages are the same. This means that link b, starting with the pinned joint as the origin, ends at the coordinates (9.89, 9.89). In addition, link c, starting from the pinned joint, ends at coordinates (4.94, -4.94).

$$L_2 \times \cos\theta = 9.89mm \tag{B.1}$$

$$L_3 \times \cos\theta = 4.94mm \tag{B.2}$$

The rotational matrix for rotating in a clockwise direction is A. B and C are the endpoint coordinates of the linkages b and c. When multiplied together, the resulting coordinates are the coordinates of the endpoint after rotating for an angle of θ.

$$A = \begin{bmatrix} \cos\theta & -\sin\theta \\ \sin\theta & \cos\theta \end{bmatrix}$$

$$B = \begin{bmatrix} 9.89 \\ 9.89 \end{bmatrix}$$

$$C = \begin{bmatrix} -4.94 \\ 4.94 \end{bmatrix}$$

Multiplying A and B gives the endpoint of b after the rotation about the pinned joint. Multiplying A by C give the endpoint of c after the rotation about the pinned joint. The coordinates for A x B are (13.98, 0.0), and the coordinates for A x C are (0.0, -6.98). By subtracting these coordinates from the original coordinates, we discover that the endpoint of b has moved about 4mm in the x direction and 10mm in the y direction. The embedded plate will mimic this movement, and one side of the plate will stay anchored while the other moves 10mm axially and up to 4mm laterally (lateral motion is limited by the polyurethane that the plate is embedded in and by the linkage system attached to the other end of the plate. Using the length of the plate and the displacement, we can again use trigonometry to calculate the angle of deflection of the plate. This angle, α, turns out to be about 28.9 degrees.

$$\alpha = \arcsin(\frac{10mm}{L_f}) \tag{B.3}$$

Bibliography

[1] Yoseph Bar-Cohen. Electroactive polymers (eaps). December 2004. http://electrochem.cwru.edu/encycl/art-p02-elact-pol.htm.

[2] David Barrett. Design of the mit robotuna. MIT Towing Tank Website. http://web.mit.edu/towtank/www/Tuna/Tuna1/design.html.

[3] David Barrett. Robotuna. MIT Towing Tank Website. http://web.mit.edu/towtank/www/Tuna/tuna.html.

[4] David Barrett. Robotuna. MIT Towing Tank Website. http://web.mit.edu/towtank/www/Tuna/Tuna1/work.html.

[5] David Barrett. Robotuna 2. MIT Towing Tank Website. http://web.mit.edu/towtank/www/.

[6] Ball bearings 101. Machine Design Website. http://www.bearings.machinedesign.com/guiEdits/Content/BDE_6_4/bdemech_a04.aspx.

[7] Sangbae Kim. Sangbae kim's biomimetic world. Stanford's Mechanical Engineering Department. http://www-cdr.stanford.edu/~sangbae/sangbae.htm.

[8] Taik-Min Lee, Dong-Yoon Lee, Ho-Cheol Lee, and Min-Yang Yang. Design of cam-type transfer unit assisted with conjugate cam and torque control cam. Modeling research, Korea Institute of Machinery and Materials, October 2008. http://www.sciencedirect.com/science?_ob=ArticleURL&_udi=B6V46-4TR97HT-1&_user=501045&_rdoc=1&_fmt=&_orig=search&_sort=d&view=c&_acct=C000022659&_version=1&_urlVersion=0&_userid=501045&md5=a17f3073d5599570563d97cc1bc838dd.

[9] Gheorghe Manolea and Alexandru Bitoleanu. Analytical determination of the d. c. motor efficiency under actual operating conditions. Computational modeling research, University of Craiova, May 2001. http://szabol0.tripod.com/WorkshopParamEM/Paper11_Manolea.pdf.

[10] Maxon motor - at a glance. Maxon Motor Corporation Website. http://www.maxonmotor.ch/ch/en/product_overview.html.

[11] Resource Manager's Office. Cordell hull fish attractor information. Army Corps of Engineers. http://www.orn.usace.army.mil/op/COR/rec/images/fish/LargemouthBass.jpg.

[12] Diane Rome Peebles. Blackfin tuna. Florida Sport Fishing Journal. http://floridasportfishing.com/magazine/species/inshore-gamefish/blackfin-tuna.html.

[13] Wilfried Stoll. Aqua ray. Festo AG and Co., Rechbergstrabe 3, 73770 Denkendorf, Germany. http://www3.festo.com/__C1256D56002E7B89.nsf/html/Aqua_ray_en.pdf/$FILE/Aqua_ray_en.pdf.

[14] Mark L. Swinson and David J. Bruemmer. Expanding frontiers of humanoid robotics. *IEEE Intelligence Systems Special Issue on Humanoid RoboticsJournal*, July 2000. http://www.inl.gov/adaptiverobotics/humanoidrobotics/pubs/special-issue.pdf.

[15] Voice coil actuators and motors. Globalspec Engineering Search Engine. http://motion-controls.globalspec.com/learnmore/motion_controls/motors/voice_coil_motors.

[16] Michael Y. Wang, Xiaoming Wang, and Shikui Chen. Topology synthesis of compliant mechanisms. Computational modeling and design laboratory, The Chinese University of Hong Kong, February 2005. http://www2.mae.cuhk.edu.hk/~cmdl/project/compliant20mechanism.htm.

[17] Pablo A. Valdivia y Alvarado. *Design of Biomimetic Compliant Devices for Locomotion in Liquid Environments.* PhD dissertation, Massachusetts Institute of Technology, Department of Mechanical Engineering, January 2007.

[18] W. Jong Yoon, Per G. Reinhall, and Eric J. Seibel. Analysis of electroactive polymer bending: A component in a low cost ultrathin scanning endoscope. Department of mechanical engineering, University of Washington, January 2006. http://www.sciencedirect.com/science?_ob=ArticleURL&_udi=B6THG-4K5HWD4-2&_user=501045&_rdoc=1&_fmt=&_orig=search&_sort=d&view=c&_acct=C000022659&_version=1&_urlVersion=0&_userid=501045&md5=387eec3bd68466cb2a551cd9124b3f12.